Proceedings of ASME Turbo Expo 2020
Turbomachinery Technical Conference and Exposition
GT2020
June 22-26, 2020, London, England

GT2020-16017

CALIBRATION OF CDM-BASED CREEP CONSTITUTIVE MODEL USING ACCELERATED CREEP TEST (ACT) DATA

Md Abir Hossain[1], Robert Mach[1], Jacob Pellicote[1], Calvin M. Stewart[1]

[1]The University of Texas at El Paso, El Paso, Texas, USA 79968-0521

ABSTRACT

In conventional creep testing (CCT) a specimen is subject to constant load and temperature for a long-duration until creep rupture occurs. Conventional testing can be costly when considering the number of experiments needed to characterize the creep response of a material over a range of stress and temperature. To predict long-term creep-rupture properties, the time-temperature-stress superposition principle (TTSSP) approach has been employed where stress and/or temperature is applied at an elevated level; the result of which are extrapolated down to low stress and/or temperature conditions. These methods have been successful in predicting minimum-creep-strain-rate (MCSR) and stress-rupture (SR) but suffer from an inability to predict the creep deformation curve or account for changes in deformation mechanisms or aging that occurs at long-duration. An accelerated technique, termed the Stepped isostress method (SSM) allows the accelerated testing of materials to determine their creep deformation response. Unlike TTSSP tests, the SSM test employs a single specimen where the stress is periodically step increased until rupture. The SSM creep deformation curve is processed (time and strain shifted) to produce an accelerated creep deformation curve that represent the creep deformation curve at the initial stress level in SSM. A processing procedure for metals has yet to be developed.

The research objective of this study is to develop a processing procedure for SSM test data using a creep-damage constitutive model. Triplicate SSM tests were conducted on Ni-based superalloy Inconel 718 at 650°C with stress being periodically increased until rupture. Triplicate CCT tests were conducted at the initial stress level of the SSM tests. The Sine-hyperbolic (Sinh) creep-damage model was employed in this study. The Sinh creep-damage constitutive model is based on coupled creep strain rate and damage evolution equations; where both rates are dependent on the current state of damage. Calibration is two-step: analytical and numerical optimization. Each stepped creep deformation curve is tackled quasi-analytically to determine MCSR and SR related material constants and accumulated damage. The damage accumulated at the end of each step was then passed onto subsequent steps to calibrate the MCSR, rupture prediction, and damage evolution. Numerical optimization was applied to optimize model constants involved in the creep strain constitutive equations in order to generate best-fitted Sinh creep deformation curves. The Sinh model predictions were compared to the SSM and CCT data. The Sinh model satisfactorily predicts the SSM data and thus the calibrated material constants provides a good estimate of rupture found in the CCT data. Calibration using SSM data reduces the number of tests needed to calibrate a model; significantly reducing costs. A single SSM test replaces numerous creep tests at different stresses.

Keywords: Creep; Inconel 718; Numerical optimization; Sine-hyperbolic model; Stepped isostress method; Time-temperature-stress superposition principle

NOMENCLATURE

$\dot{\varepsilon}_{\min}$	minimum-creep-strain-rate
$\dot{\varepsilon}_{final}$	final-creep-strain-rate
t_r	rupture time
CSR	creep-strain-rate
CCT	Conventional creep test
MCSR	Minimum-creep-strain-rate
FCSR	Final-creep-strain-rate
SIM	Stepped isothermal method
SR	Stress-rupture
SSM	Stepped isostress method
TTSSP	Time-temperature-stress-superposition principle

1. INTRODUCTION

1.1 Motivation

The development of new candidate alloys to improve the efficiency and performance of turbomachinery has a high cost.

To gather creep performance data, there is a requirement to perform conventional creep tests (CCTs). The ASME B&PV III code outlines stringent requirements for the approval of new materials where each heat of a material must be tested to 10000+ hours; 30000+ hours based on the stability of strengthening microstructure) [1]. According to Haynes International, the average time to implement of a new creep resistant alloy is between 10 to 20 years [2]. There is an urgent need for accelerated creep tests (ACTs) that enable the rapid evaluation of candidate creep-resistant materials and the down selection to the best candidates for further CCT testing [3]. In this study, an accelerated creep test (ACT) called the stepped isostress method (SSM) was evaluated for metallic materials.

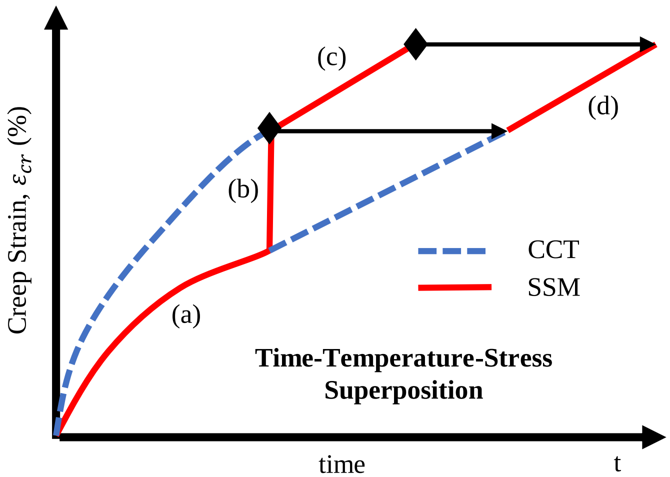

Figure 1: Time-temperature-stress superposition principle (TTSSP) visualization of (a) reference stress or temperature level, (b) stress or temperature step, (c) elevated stress or temperature level, and (d) accelerated creep strain

1.2 Time-Temperature-Stress Superposition (TTSSP)

Time-temperature-stress superposition (TTSSP) theory states there exists a fundamental relationship between time, temperature, and stress which can be manipulated to reduce testing duration [4]. The TTSSP concept for creep deformation is that the creep-strain-rate of a test conducted at higher temperature and/or stress can be time-shifted to match that of a conventional test conducted at service conditions. With TTSSP, multiple temperature and stress increases can be applied during a single experiment (Figure 1). While both temperature and stress increases can be performed simultaneously, they are often segregated into two test types: stepped isothermal method (SIM) and stepped isostress method (SSM) respectively where during a single experiment multiple isotherms or isostresses are applied. There is a choice to apply temperature or stress increase for acceleration. Temperature increase accelerates the metallurgical/chemical changes (phase transformation, carbide precipitation, and coarsening etc.) while the stress increases accelerate mechanical changes (grain boundary sliding, creep cavitation etc.). The stepped isothermal method (SIM) is often applied where temperature is step increased while load is fixed until rupture [5]. A single specimen is needed to run a SIM test. The choice of temperature level, the number of steps, and hold time control the duration of a SIM test. The creep deformation curve exhibit different creep-strain-rates during each hold time in a SIM conducted test. A single conventional creep curve corresponding to the lowest temperature and fixed stress applied during the tests can be constructed via mathematical processing.

Instead of varying temperature, the applied load is varied and this approach is termed the stepped isostress method (SSM) [6]. In SSM, stress is stepped increased while temperature is fixed until rupture. The relationship among CCT, SIM, and SSM resolves into following

Conventional **SIM** **SSM**

$$\dot{\varepsilon}_{cr}(\sigma_i, T_i, t) = \dot{\varepsilon}_{cr}\left(\sigma_i, T_{i+1}, \frac{t}{\phi_{i+1}}\right) = \dot{\varepsilon}_{cr}\left(\sigma_{i+1}, T_i, \frac{t}{\phi_{i+1}}\right) \quad (1)$$

where $\dot{\varepsilon}_{cr}$ is creep strain rate at the service temperature, T_i and stress, σ_i and the stepped increases of temperature and stress are T_{i+1} and σ_{i+1} respectively. The rate match is achieved by introducing a time-shift factor, ϕ_{i+1} to time. Multiple stepped increases of temperature and/or stress can be performed in a single specimen with each step requiring both a distinct time-shift factor, ϕ_{i+1} and virtual start time, $t_{0,i+1}$.

The SIM and SSM tests have been performed successfully and extensively on polymers and polymeric composites [7-15]. Experimentally, SSM is the preferred because load control is easier than temperature control; and virtually little difference is observed between SIM and SSM tests in polymers due to the relatively simple creep mechanisms (when compared to metals). Moreover, SSM does not need to use the elevated temperatures; chemical properties of the tested materials are not affected and the problem concerning the slow and non-uniform heating is avoided. A parameter termed acceleration ratio is used to infer the ranges of extrapolated creep response. The acceleration ratio, A can be defined as

$$A = \frac{t_r(\sigma_1)}{t_{SSM}} \quad (2)$$

where, t_r is the extrapolated rupture time at initial stress and t_{SSM} is the rupture time of SSM test. Jazouli performed nine 1-hr SSM tests on Polycarbonate at different stress levels and calculated acceleration ratios up to 3 log [7]. Luo studied several poly blends, performed SSM tests at different stresses, and achieving acceleration ratios of 2 log [8-9]. Giannopoulos et al. studied the SSM testing of the technical fibers (Kevlar 49 and technical yarns) with the acceleration ratio of 6.5log [11]. Tanks et al. applied the SSM on unidirectional Carbon Fiber Reinforced Plastic (CFRP) laminates where creep response was successfully predicted up to acceleration ratio of 3log [13]. In a separate study by Tank et al. where SSM was employed on the transverse CFRP laminates where accurate prediction on creep response was done up to acceleration ratio of 3log [14]. Fairhurst et al. applied SSM on polyetheretherketone (PEEK), polyetherimide (PEI), and polyamideimide (PAI) polymeric compounds to accurately predict the creep response to over acceleration ratio of 2log [15]. The multistep SSM approaches have shown great success for polymers and polymeric composites in predicting the long-term creep behavior. However, these approaches have never been applied to metallic materials where creep deformation mechanisms are complex and function of stress and temperature.

1.3 Problem Statement

Past work has been successful in determining the creep response of polymer and polymeric composites through the application of SSM. Very little has been achieved in terms of metallic materials or super alloys in the prior studies. A method for calibration of SSM data for metallic materials is needed. The deformation mechanism of metallic materials are complex and the simplistic method to process the SSM data for polymers are not appropriate. Continuum damage mechanics (CDM) based Sine-hyperbolic (Sinh) model have been successful in extrapolating creep deformation, minimum-creep-strain-rate, and stress-rupture of CCTs [16-18]. The CDM-based Sinh model are more advantageous as it relates to processing SSM data

- An analytical method is applied for finding most of the material constants.
- Coupled differential equations can be analytically manipulated to account for stepped increase of loading.

It is hypothesized that CDM-based creep models can be employed to process SSM data into creep deformation curves that predict the CCT response of metallic materials.

2. OBJECTIVES

The objective of this study is to demonstrate the processing of metallic SSM data into CCT predictions using the CDM-based Sinh creep-damage model. The SSM and CCT tests were conducted on Ni-based superalloy Inconel 718 at 650°C. The CDM-based Sinh model is introduced. An analytical approach to the calibration of Sinh to SSM data is derived where the derived equations are used to obtain initial-guess constants that are refined using numerical methods to obtain best-fit to the data. Simulations of CCTs are made using the calibrated Sinh model. A qualitative and quantitative comparison is made between the Sinh predictions and the real CCTs performed separately. Finally, conclusions are made concerning the accuracy of Sinh for processing of metallic SSM data.

3. MATERIALS AND TEST METHODS

3.1 Alloy Inconel 718

The subject material in this study is non-heat treated (NHT) Inconel 718. Inconel 718 is a nickel-based superalloy consisting of a gamma γ-Ni (FCC) matrix strengthened by γ'-$Ni_3(Al,Ti)$ and γ''-Ni_3Nb (BCT) precipitates particles [19]. The material was received as 0.5 in diameter round bar prepared to AMS 5662 [20]. The heat was melted using the VIM and ERS process. At the mill the ingot was solution annealing at 955°C for 1 hour and water quenched. The nominal and mill test report (MTR) chemical composition of IN718 are provided in Table 1. A finishing heat-treatment was not performed on the material; therefore, this material should be considered as Non Heat Treated (NHT). Specimens were machined with a gage length of 25.4 mm and diameter of 6.35 mm. Specimens were prepared according to ASTM E8 and ASTM E139 standard [21-22].

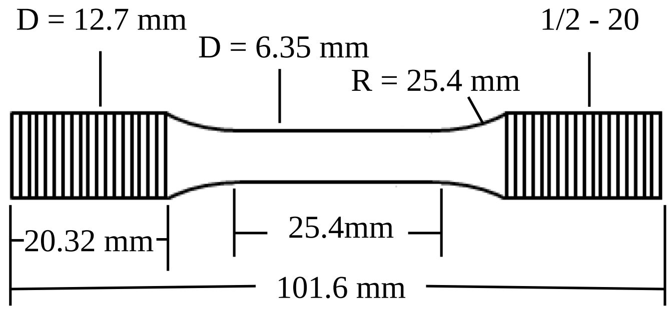

Figure 2: Specimen dimensions in mm tolerances of 0.0254 mm.

Table 1: Chemical composition (wt%) of IN 718

Element	Maximum	MTR
Ni	50-55	52.55
Cr	17-21	18.52
Fe	Bal*	18.2
Nb	4.75-5.50	5.2
Mo	2.80-3.30	2.92
Ti	0.65-1.15	0.93
Al	0.20-0.80	0.52
Co	1	0.52
C	0.08	0.04
Mn	0.35	0.05
Si	0.35	0.08
P	0.015	0.007
S	0.015	0.0005
B	0.006	0.004
Cu	0.3	0.05

A schematic of the specimen is provided in Figure 2. The SSM and CCT tests were performed according to ASTM E139 standard [22]. Mechanical tests were performed using an Instron 5969 UTM with a 50 kN load cell, an Epsilon 7650A high temperature high precision extensometer, and an ATS three-zone split-tube furnace as shown in Figure 3. The extensometer meets ASTM E83 class A with a 1 in gauge section and measures up to 10% strain [23]. The strain rate for the tensile tests were 0.001 mm/mm/s. The furnace has three zones and is controlled using the Watlow PM digital controller. A K-type thermocouple is welded to the center of the gauge section of each specimen using a HotSpot II thermocouple welder and monitored using a CSi32 Omega Miniature Benchtop Controller. Monotonic tensile tests were performed on three specimens at 650°C with the average tensile properties reported in Table 2.

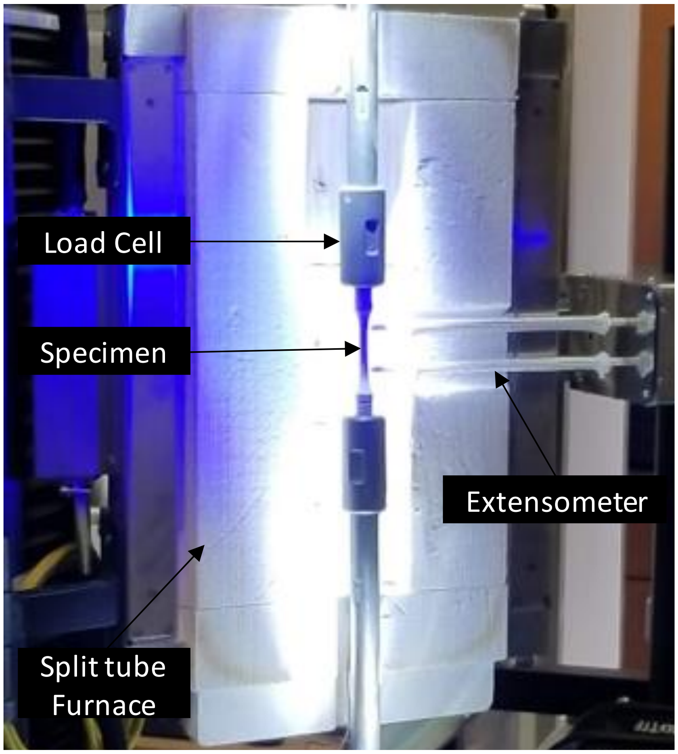

Figure 3: Test setup for stepped isostress method (SSM) and conventional creep tests (CCT)

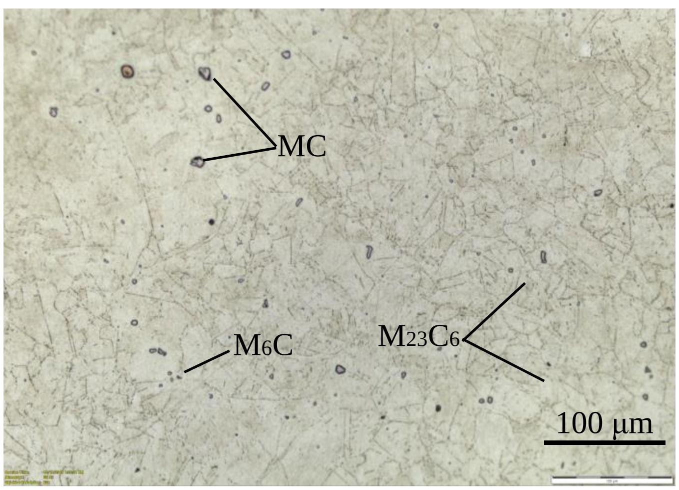

Figure 4: Microstructure of IN718 specimen prepared for testing

Table 2: Tensile properties of IN 718 at 650°C

Property	Value
Yield Stress (MPa)	634.4
Ultimate Tensile Strength (MPa)	824.4
Young's Modulus (GPa)	152.7

The micrograph of the prepared IN 718 specimens for testing is shown in Figure 4. The microstructure is at 20x magnification and etched with agent Kalling's No 2. This etchant relieves γ' and reveals the existing grain boundaries using 5 g $CuCl_2$, 100 mL of HCl, and 100 mL Ethanol. The MC carbides are typically larger and have very angular morphologies. These carbides also have a tint of pink ultimately revealing molybdenum or tungsten as the metal element of the MC carbide. The M_6C carbide has a round morphology and is found at grain and twin boundaries. the $M_{23}C_6$ carbides are seen defined by a blocky morphology within the grain boundaries themselves.

The initial hold time for SSM are established using the experimental TTT and TTP diagrams for IN718. Transitions occur between the γ ↔ γ′+γ", γ′+γ" ↔ α-Cr, and α-Cr ↔ σ regions at approximately 100, 1000, and 10000 hours respectively. Carbide precipitation is not expected at 650°C for up to 1000 hours. These transition times inform the initial hold time. The intermediate hold time was set to minimum of 5 hours. The number of stress levels for SSM test were set to 4. The tests were performed well above the 0.2% yield strength of alloy IN 718 at 650°C. The SSMs were load controlled. The specimen was subjected to loading over yield strength likely to deform plastically. The instantaneous plasticity of repeated yielding was the likely source for reduced rupture life and increased ductility. Combination of creep damage and plastic damage accelerate the deformation mechanisms in the SSM tests that lead to damage accumulation at a much higher rate than the CCTs. The test matrix for the SSM test conducted are reported in Table 3.

Table 3: SSM test matrix for alloy IN 718

Temperature (°C)	Stress, σ (MPa)	Hold Time, (hr)	Estimated Acceleration Ratio, A
650	636	5.00	4.55x
650	681	5.00	2.62x
650	726	5.00	1.51x
650	771	21.86	0.88x

4. SINE-HYERBOLIC (SINH) MODEL

The Sine hyperbolic (Sinh) CDM-based model was developed to model the secondary and tertiary creep stages of a typical creep curve [24-27]. The Sinh model consists of a creep-strain-rate (CSR) and damage evolution equation as follows

$$\dot{\varepsilon}_{cr} = A\sinh\left(\frac{\sigma}{\sigma_s}\right)\exp(\lambda\omega) \tag{3}$$

$$\dot{\omega} = \frac{M(1-\exp(-\phi))}{\phi}\sinh\left(\frac{\sigma}{\sigma_t}\right)^{\chi}\exp(\phi\omega) \tag{4}$$

where A, σ_s, λ, M, σ_t, and χ are material constants, σ is stress, and ω is damage; an internal state variable that evolves from an initial damage to unity. Previous version of the Sinh model included a 3/2 power on the exponential term in [Eq. (3)] [16-18,24-25]. The slightly modified version of the model removing the power term is used in this study to achieve a closed-form solution and faster convergence in FEA analysis. Assume that initial damage is zero, $\omega_o = 0$. The secondary creep material constants A and σ_s can be calibrated as

$$\dot{\varepsilon}_{\min} = A\sinh\left(\frac{\sigma}{\sigma_s}\right) \tag{5}$$

where $\dot{\varepsilon}_{\min}$ is the minimum-creep-strain-rate (MCSR) measured from creep data. The constant λ is unit-less and analytically derived to be

$$\lambda = \ln\left(\frac{\dot{\varepsilon}_{final}}{\dot{\varepsilon}_{\min}}\right) \tag{6}$$

where $\dot{\varepsilon}_{final}$ is the final-creep-strain-rate (FCSR) measured from creep data. The λ constant may exhibit stress and/or temperature dependence. Integration of [Eq. (4)] furnishes damage, ω and rupture, t_r predictions as follows

$$\omega(t) = -\frac{1}{\phi}\ln\left[1-\left[1-\exp(-\phi)\right]\frac{t}{t_r}\right] \tag{7}$$

$$t_r = \left[M\sinh\left(\frac{\sigma}{\sigma_t}\right)^{\chi}\right]^{-1} \tag{8}$$

where initial time, t_o is set to zero. Damage [Eq. (7)] depends on the ϕ material constant and rupture predictions [Eq. (8)]. The ϕ constant controls the damage trajectory and may be stress and/or temperature dependent. The rupture prediction [Eq. (8)] depends on the M , σ_t , and χ material constants. The material constant σ_t facilitates the transition from the low-stress to high-stress regime.

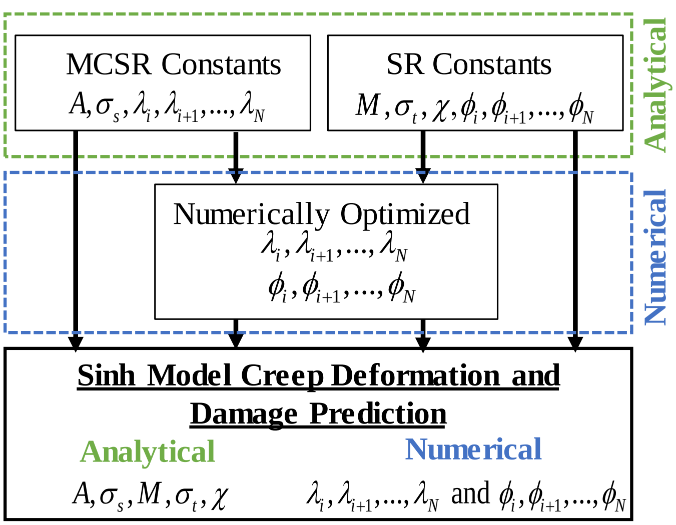

Figure 5: An illustration of the calibration approach by Sinh model for SSM test data.

5. RESULT AND DISCUSSION

5.1 Material Constant Calibration

Calibration of the Sinh model material constants is performed to portray the accuracy of the Sinh in predicting the creep deformation to rupture. The calibration of the SSM test data begins with the determination of the material constants in the Sinh coupled constitutive equation. The Sinh model take 7 material constants $(A, \sigma_s, \lambda, M, \sigma_t, \chi, \phi)$ into the constitutive equations. An illustration of the calibration approach adopted in this study is shown in Figure 5. The calibration approach is twofold: Analytical and Numerical.

5.2 Minimum-Creep-Strain-Rate Constant

The first step of the calibration approach is the determination of MCSR related constants. Sinh CSR equation [Eq. (3)] for SSM is can be stated as follows

$$\dot{\varepsilon}_{cr} = A\sinh\left(\frac{\sigma_i}{\sigma_s}\right)\exp(\lambda_i\omega) \tag{9}$$

where, i denotes the stress level of interest. Material constant A and σ_s are scalar and assumed to be independent of stress or damage variation. Material constant λ is a vector (variable as step changes) and dependent of stress and/or damage accumulation. CDM-laws state that, at the beginning damage is zero $(\omega = 0)$ and at the rupture damage reached to unity $(\omega = 1)$. These two states are exploited to form the following equations

$$\dot{\varepsilon}_{\min} = A\sinh\left(\frac{\sigma_1}{\sigma_s}\right) \tag{10}$$

$$\dot{\varepsilon}_{final} = A\sinh\left(\frac{\sigma_N}{\sigma_s}\right)\exp(\lambda_N) \tag{11}$$

$$\lambda_N = \ln\left(\frac{\dot{\varepsilon}_{final}}{\dot{\varepsilon}_{\min}}\right) \tag{12}$$

where, N denotes material constants at the final stress level and σ_1 is the initial stress. Minimum $(\dot{\varepsilon}_{\min})$ and final $(\dot{\varepsilon}_{final})$ creep strain rate are determined directly from the experimental data. These 3 equation are solved analytically to find the material constant A, σ_s , and λ_N. Next step is to calibrate the remaining material constant, λ and damage vector, ω across the stress levels. The Sinh CSR equation [(3)] is rearranged to the following form.

$$\lambda_i\omega = \ln\left(\frac{\dot{\varepsilon}_{cr}}{A\sinh\left(\frac{\sigma_i}{\sigma_s}\right)}\right) \tag{13}$$

The non-separable $\lambda_i\omega$ is calculated with employing the [Eq. (13)]. The λ and ω is separated and a simulated magnitude is calibrated for each of λ and ω. An objective function is employed to optimize the simulated value for λ and ω setting the following constraint.

$$\begin{aligned} &\lambda_i > \lambda_{i-1} > \ldots > \lambda_N \\ &0 \le \lambda_i \le \ln(\infty) \\ &0 \le \omega \le 1 \end{aligned} \tag{14}$$

The analytically calibrated MCSR related material constants are reported in Table 4. Note that, the analytically evaluated material constant, λ is later numerically refined to fit the model through the data.

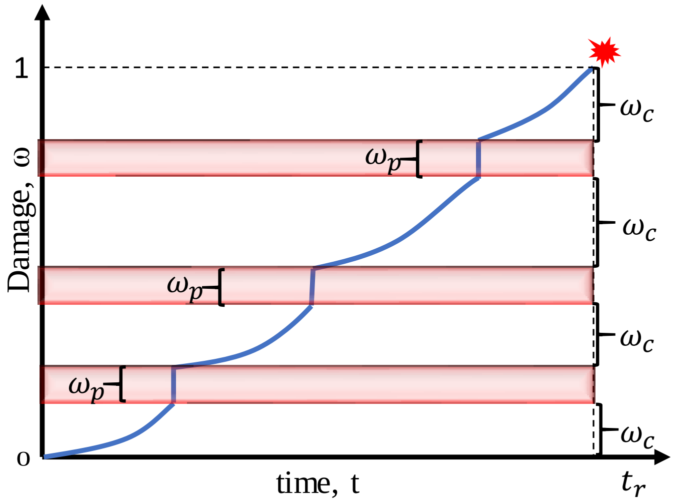

Figure 6: An illustration of plastic damage and creep damage accumulating during SSM test

5.3 Stress Rupture Constants

In this section the SR related material constants are calibrated. The first step is to generate the damage evolution curve. The damage curve can be obtained using the calibration approach adopted in the previous section. An illustration of the likelihood of the damage evolution curve is shown in Figure 6. The shaded region in Figure 6 is the instantaneous plastic damage that occurs during the load steps. The sudden introduction of this plastic damage has the effect of reducing the creep resistance of the material. For each SSM test, final damage accumulation is the sum of creep and instant plastic damage.

The next step is to employ the Sinh damage rate equation [Eq. (4)] to calibrate the SR related material constants. Sinh damage rate equation [Eq. (4)] can be stated as follows for SSM

$$\dot{\omega} = \frac{M[1-\exp(-\phi_i)]}{\phi_i} \sinh\left(\frac{\sigma_i}{\sigma_t}\right)^{\chi} \exp(\phi_i \omega) \tag{15}$$

where, i denotes the stress level of interest. Material constant M, σ_t, and χ are scalar and assumed to be independent of stress and/or damage accumulation. Material constant, ϕ_i is vector and dependent of the stress and/or damage accumulation. A similar framework is developed here like the previous section to calibrate SR related material constant. Exploiting the CDM laws, the following 4 equations can be formulated

$$\omega_{c,1} = -\frac{1}{\phi} \ln \left[1 - [1-\exp(-\phi)] \frac{t_1}{\left[M \sinh\left(\frac{\sigma_1}{\sigma_t}\right)^{\chi} \right]^{-1}} \right] \tag{16}$$

$$\dot{\omega}_o = \frac{1-\exp(-\phi_1)}{\phi_1} M \sinh\left(\frac{\sigma_1}{\sigma_t}\right)^{\chi} \tag{17}$$

$$\dot{\omega}_f = \frac{1-\exp(-\phi_N)}{\phi_N} M \sinh\left(\frac{\sigma_N}{\sigma_t}\right)^{\chi} \exp(\phi_N) \tag{18}$$

$$\phi_N = \ln\left(\frac{\dot{\omega}_o}{\dot{\omega}_f}\right) \tag{19}$$

where, N denotes the materials constants at the final stress level, $\omega_{c,i}$ is creep damage accumulated at the first step, $\dot{\omega}_o$ and $\dot{\omega}_f$ is the initial and final damage rate respectively, and σ_1 is the stress level of first step.

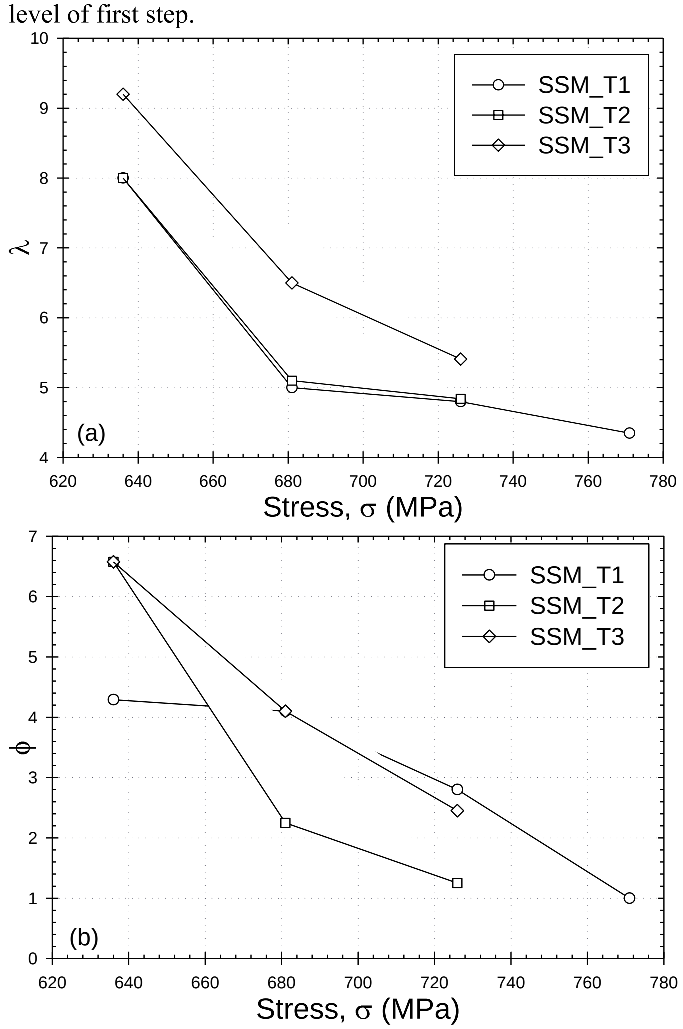

Figure 7: Calibrated (a) λ and (b) ϕ for triplicate SSM across multiple stress at 650°C

To calibrate the material constant ϕ_1, [Eq.(16)] and [Eq. (17)] are combined and rearranged to following form

$$\omega_{c,1} = -\frac{1}{\phi}\ln\left[1-\left[1-\exp(\phi)\right]\frac{t_1\phi_1\dot{\omega}_o}{1-\exp(-\phi_1)}\right] \qquad (20)$$

Solving [Eq. (20)], the material constant ϕ_1 is calibrated.

The remaining equation [Eq. (16)-(19)] are solved to calibrate the material constant, M, σ_t, χ, and ϕ_N by setting the following constraints.

$$\begin{aligned} &\phi_i > \phi_{i-1} > \ldots > \phi_N \\ &0 \le \phi_i \le \ln(\infty) \\ &0 \le \sigma_t \le \sigma_{UTS} \\ &M>0 \end{aligned} \qquad (21)$$

The analytically calibrated material constants are reported in Table 4. To find the intermediate ϕ constants $(\phi_{i+1}, \phi_{i+2}, \ldots, \phi_{N-1})$, a numerical approach is adopted. An objective function is employed and optimized to find the best-fitted ϕ for each load steps.

The numerically refined material constants, λ and ϕ for triplicate SSM test are plotted to illustrate the strong stress dependency in Figure 7. Both λ and ϕ show a decreasing trend with the increasing stress. For material constant, λ at high stress FCSR approaches to MCSR leading to higher ductility and shorter rupture life. On the other hand, at high stress material constant ϕ is required to decrease to facilitate the damage evolution a shorter trajectory.

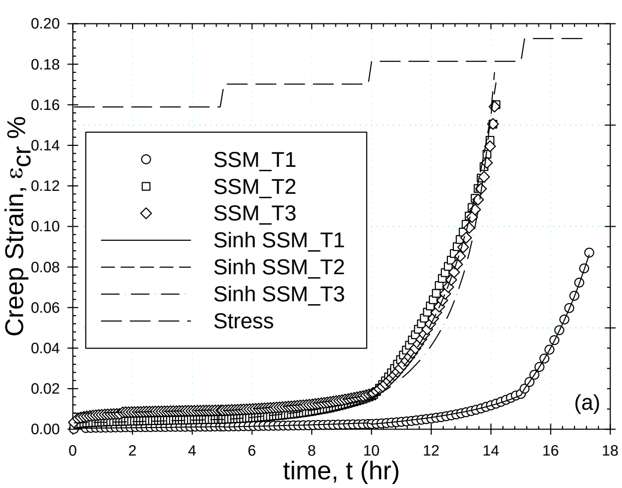

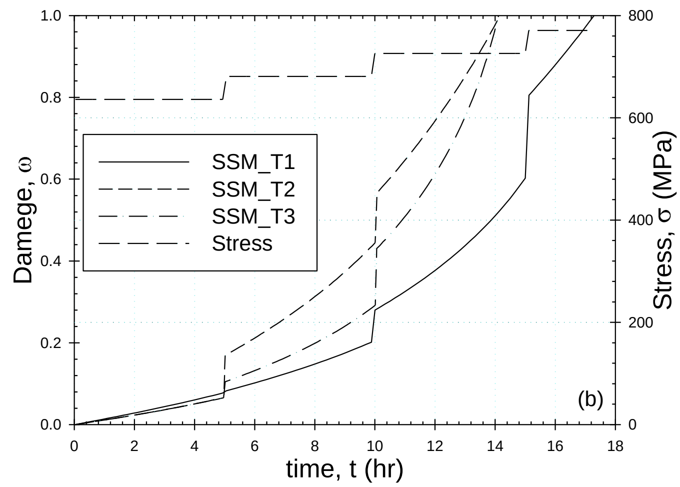

Figure 8: Sinh model estimation of (a) creep deformation and (b) damage evolution for triplicate SSM test at 650°C

5.4 Calibration Result

The calibrated material constants are provided to Sinh constitutive equation to generate Sinh predicted creep deformation and damage evolution curves. The Sinh CSR equation [Eq. (3)], damage rate equation [Eq. (4)] are used to calibrate the rate. The following equation is used to determine the creep strain at each time step.

$$\varepsilon_{cr,i} = \dot{\varepsilon}_{cr,i}.\Delta t + \varepsilon_{cr,i-1} \qquad (22)$$

where, $\varepsilon_{cr,i}$ and $\dot{\varepsilon}_{cr,i}$ is the creep strain and creep strain rate at current step, $\varepsilon_{cr,i-1}$ is the creep strain at previous step, and Δt is the time stepping of each iteration. Note that, time stepping, Δt is 0.16 hr. The material constants λ and ϕ are switched at each stress levels.

The Sinh creep deformation and damage prediction for the SSM test is shown in Figure 8. The Sinh fit accords well with the experimental SSM data. The model also exhibits the ability to predict the damage evolution from zero to unity across multiple stresses. The damage evolution curves show instantaneous plasticity attributed to repeated yielding of the test specimen. This introduction of plastic damage along with the creep damage leads to quick rupture of the specimen; leading to shorter test duration. The Sinh model damage prediction accounts for the induced plastic damage as shown in the Figure 8.

Table 4: Analytically calibrated material constants of Sinh model for triplicate SSM at 650°C

Test ID	A $\%hr^{-1}\times10^{-7}$	σ_s MPa	M $hr^{-1}\times10^{-2}$	σ_t MPa	χ
SSM_T1	1.52	86.35	5.80	834.40	13
SSM_T2	3.83	87.58	6.90	834.40	13
SSM_T3	3.52	86.77	7.60	834.40	13

The quantitative comparison of creep damage versus instantaneous plastic damage induced by stepped increase in stress in triplicate SSM test is presented in Table 5. The instantaneous plastic damage induced in each of SSM test ranges from 28.66% to 17.64% of the total damage. On average, this represents almost one-fifth of the total life of a specimen is being damaged by the instantaneous plastic damage. This calibration approach demonstrates that the Sinh model can fit the experimental creep curves conducted by SSM given the correct set of material constants.

Table 5: Percentage of creep damage and instantaneous plastic damage in SSM at 650°C

Test ID	Creep Damage (%)	Instant Plastic Damage (%)
SSM_T1	71.34	28.66
SSM_T2	77.52	22.48
SSM_T3	82.36	17.64

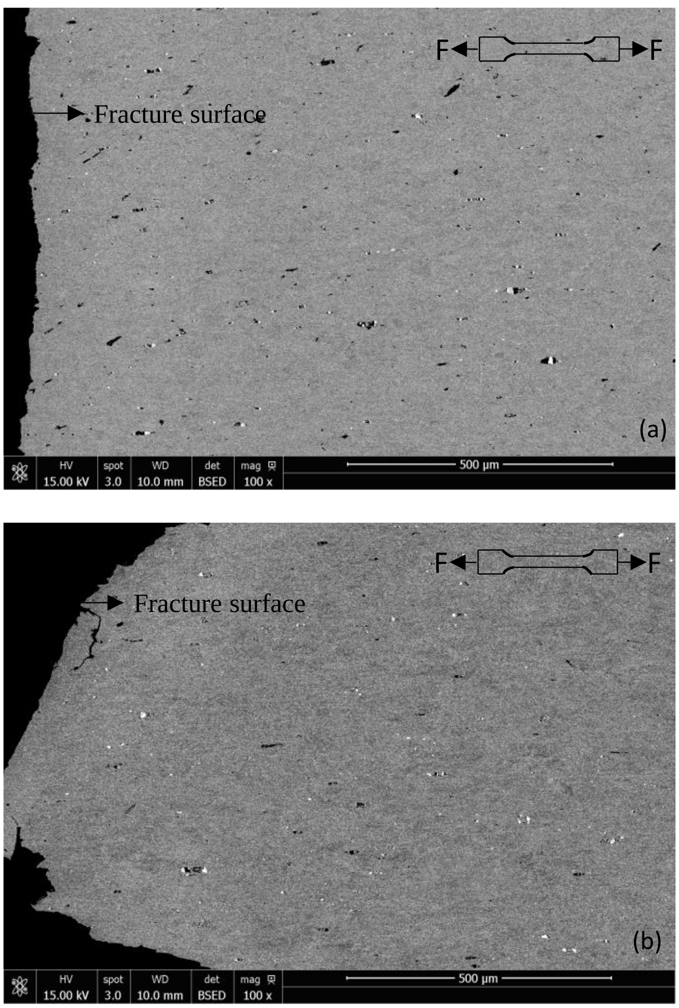

Figure 9: Micrograph of fracture surface of failed specimen for the (a) CCT and the (b) SSM tests.

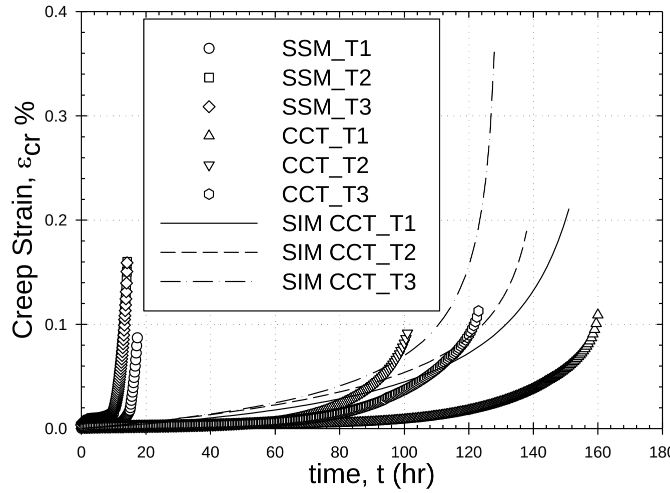

Figure 10: Comparison of Sinh extrapolated CCTs with experimental CCTs and SSMs

5.5 Post-Audit Validation

The micrograph of the fracture surface of failed specimen from a CCT and SSM test in shown in Figure 9. The micrographs are taken by a Quanta Fei 650 SEM. The fracture surface by SSM clearly show the necking of the specimen due to rapid loading compared to the CCT specimen. Cavity creation and crack propagation is the dominant failure mechanism in case of the accelerated creep test. To validate the proposed method analytically, the Sinh model is applied to extrapolate the simulated CCTs at reference stress. Calibrated material constant at section 5.2 and 5.3 are employed. The Sinh rupture time prediction equation [Eq. (8)] is employed to determine the rupture time. The reference stress is applied for extrapolating the simulated CCTs. In this study, size of time stepping is taken as 1 hr. To make the creep deformation prediction, [Eq. (3) & (22)] and the material constants corresponding to the initial stress level are employed. The Sinh extrapolated CCTs are compared with the experimental CCTs as shown in Figure 10. The Sinh predicted CCTs accords well with the experimental CCTs. The extrapolated creep ductility to rupture remain well within the bounds of the experimental CCTs. On average, the extrapolated CCTs show 60% higher final strain than the experimental CCTs. On the other hand, average rupture time of extrapolated CCTs are 7.19% higher than experimental CCTs. The range of rupture time of extrapolated CCTs are 37% less than the experimental CCTs. This verifies the Sinh extrapolated CCTs show consistency in estimating the rupture time while show a degree of inconsistency in estimating the creep ductility. The potential reason of this discrepancy between the model prediction and real test is the assumption made while calibrating the material constants. The material constants are assumed to be independent of stress, damage and/or micro-structural degradation. The complex plasticity versus creep mechanism in metallic materials could affect the model's constants rendering the necessity to account for re-tuning the model parameters. Moreover, the

Table 6: Final creep strain and rupture time of SSMs, CCTs, and Sinh extrapolated CCTs

Test ID	SSM ε_{cr} (%)	SSM t_r (hr)	CCT ε_{cr} (%)	CCT t_r (hr)	Sinh CCT ε_{cr} (%)	Sinh CCT t_r (hr)	Acceleration Ratio
T1	0.08	17.29	0.10	159.99	0.21	151.08	8.73x
T2	0.16	14.16	0.09	100.99	0.18	137.97	9.74x
T3	0.15	14.12	0.11	122.99	0.36	127.87	9.05x

calibrated MCSR related material constants are more sensitive than SR related material constant as little variation in the calibrated values lead to big variation in creep ductility. The final creep strain and rupture time of SSMs, CCTs, and Sinh simulated CCTs reported in Table 6. Sinh model shows credible extrapolation capability by estimating creep deformation data up to 9.5 times the actual test duration. This presents a novel pathway to calibrate the SSM test data avoiding the associated empiricism in the calibration process.

6. CONCLUSIONS

The objective of this study was to employ a CDM-based creep model to calibrate the ACT data. Triplicate SSM tests were conducted at 650°C. The Sinh model is employed to calibrate the ACT data and investigated for the extrapolation credibility. The SSM test data calibration approach by using CDM-based Sinh creep-damage model described in this paper has led to following insights:

- The twofold calibration exercise reveals that determined material constants (λ, ϕ) are susceptible to stress variation. A strong stress dependency is observed in MCSR (λ) and SR (ϕ) related material constant.
- The sudden stepped increase in loading induce plastic damage into the test specimen instantaneously. This plastic damage accounts for one-fifth of the lifetime of the specimen. The induced plastic damage coupled with creep damage lead the specimen to quick rupture, shortening the test duration. Though the specimen is subjected to plastic damage, the fidelity of the calibrated material constant by Sinh remain intact. Besides, Sinh model damage prediction accounts for the plastic damage in the damage trajectory.
- The Sinh can predict the SSM data with a high level of accuracy. The damage prediction evolves from zero to unity at rupture.
- The extrapolation credibility of Sinh is revealed the model's capability of extrapolating creep data up to 9.5 times the duration of test. The goodness of fit between extrapolated CCTs and experimental CCTs can be satisfactory for comparisons among candidate materials.
- The calibration approach resorted to in this paper assumes the model constants remain unaffected by instantaneous plastic damage, boundary condition change (stress variation), and micro-structural degradation. As creep mechanism is a complex process for metallic materials and superalloys and function of temperature and stress, the Micro-structural degradation and boundary condition variability could potentially influence the model constants. In future study, effects of these aspect on the material constants and model performance will be investigated.

The employment of CDM-based Sinh creep-damage model to calibrate the SSM test data to extrapolate long term creep response for the newer candidate materials would open a pathway for the mechanical quantification in significantly shorter time span; avoiding the empiricism of the existing approaches.

FUTURE WORK

The prospects for future work in this field of study are many. The triplicate SSMs studied in this paper presents an uncertainty in creep deformation to rupture. The experimental evidence suggests that estimation of creep deformation and rupture should be treated as a probabilistic problem. Future studies will be directed towards inclusion of probabilistic features into deterministic framework to have a more reliable and durable creep deformation to rupture estimation.

ACKNOWLEDGEMENTS

The work was supported by the Department of Energy National Energy Technology Laboratory under Award Number(s) DE-FOA-0001715.

REFERENCES

[1] ASME, 2014, *ASME Boiler and Pressure Vessel Code, Section III, Division 1, Subsection NS - Class - 1, Components in Elevated Temperatures Service,* New York, NY.

[2] Council, N. S., 2016, *Advanced Manufacturing: A Snapshot of Priority Technology Areas Across the Federal Government Subcommittee for Advanced Manufacturing*.

[3] Miracle, D., Majumdar, B., Wertz, K., and Gorsse, S., 2017, "New Strategies and Tests to Accelerate Discovery and Development of Multi-Principal Element Structural Alloys," Scr. Mater., **127**, pp. 195–200.

[4] Tobolosky, A., and Eyring, H., 1943, "Mechanical Properties of Polymeric Compounds," J. Chem. Phys., 11(3), pp. 125–134.
[5] Thornton, J. S., Paulson, J. N., and Sandri, D., 1998, "Conventional and Stepped Isothermal Methods for Characterizing Long Term Creep Strength of Polyester Geogrids," *Sixth International Conference on Geosynthetics*, Atlanta, USA, pp. 691–698.
[6] Giannopoulos, I. P., and Burgoyne, C. J., 2009, "Stepped Isostress Method for Aramid Fibers," 9th Int. Symp. Fibre Reinf. Polym. Reinf. Concr. Struct., (July), pp. 15–18.
[7] Jazouli, S., Luo, W., Brémand, F., and Vu-Khanh, T., 2006, "Nonlinear Creep Behavior of Viscoelastic Polycarbonate," J. Mater. Sci., **41**(2), pp. 531–536.
[8] Luo, W., Wang, C., and Zhao, R., 2007, "Application of Time-Temperature-Stress Superposition Principle to Nonlinear Creep of Poly(Methyl Methacrylate)," Key Eng. Mater., **340**-**341 II**, pp. 1091–1096.
[9] Luo, W. B., Wang, C. H., and Zhao, R. G., 2007, "Application of time-temperature-stress superposition principle to nonlinear creep of poly (methyl methacrylate)," *Key Engineering Materials*, **340**, pp. 1091-1096.
[10] Giannopoulos, I. P., and Burgoyne, C. J., 2011, "Prediction of the Long-Term Behaviour of High Modulus Fibres Using the Stepped Isostress Method (SSM)," J. Mater. Sci., **46**(24), pp. 7660–7671.
[11] Giannopoulos, I. P., and Burgoyne, C. J., 2009, "Stepped Isostress Method for Aramid Fibers," 9th Int. Symp. Fibre Reinf. Polym. Reinf. Concr. Struct., (July), pp. 15–18.
[12] Hadid, M., Guerira, B., Bahri, M., and Zouani, A., 2014, "Assessment of the Stepped Isostress Method in the Prediction of Long Term Creep of Thermoplastics," Polym. Test., **34**, pp. 113–119.
[13] Tanks, J., Rader, K., Sharp, S., and Sakai, T., 2017, "Accelerated Creep and Creep-Rupture Testing of Transverse Unidirectional Carbon/Epoxy Lamina Based on the Stepped Isostress Method," Compos. Struct., **159**, pp. 455–462.
[14] Tanks, J. D., Rader, K. E., and Sharp, S. R., 2016, "Acclerated Creep Testing of CFRP with the Stepped Isostress Methos," Mech. Compos. Multi-functional Mater., **7**, pp. 397–403.
[15] Fairhurst, A., Thommen, M., and Rytka, C., 2019, "Comparison of Short and Long Term Creep Testing in High Performance Polymers," Polym. Test., **78**(July), p. 105979.
[16] Haque, M. S., and Stewart, C. M., 2016, "Finite-Element Analysis of Waspaloy Using Sinh Creep-Damage Constitutive Model Under Triaxial Stress State," J. Press. Vessel Technol. Trans. ASME, 138(3), pp. 1–9.
[17] Haque, M. S., and Stewart, C. M., 2017, "The Stress-Sensitivity, Mesh-Dependence, and Convergence of Continuum Damage Mechanics Models for Creep," J. Press. Vessel Technol. Trans. ASME, **139**(4), pp. 1–10.
[18] Hossain, M. A., and Stewart, C. M., 2019, "Reliability Prediction of 304 Stainless Steel Using Sine-Hyperbolic Creep-Damage Model with Monte Carlo Simulation Method," *Proceedings of ASME 2019 Pressure Vessel and Piping Conference PVP2019*, San Antonio, Texas, USA.
[19] Ni, T., and Dong, J., 2017, "Creep Behaviors and Mechanisms of Inconel718 and Allvac718plus," Mater. Sci. Eng. A, **700**(June), pp. 406–415.
[20] AMS F Corrosion Heat Resistant Alloys Committee, 1965, "Nickel Alloy, Corrosion and Heat Resistant, Bars, Forgings, and Rings 52.5Ni 19Cr 3.0Mo 5.1Cb 0.90Ti 0.50Al 18Fe, Consumable Electrode or Vacuum Induction Melted 1775°F (968°C) Solution Heat Treated, Precipitation Hardenable."
[21] Standard Test Method for Tension Testing of Metallic Materials, August (2013), DOI: 10.1520/E0008_E0008M-13A
[22] American Society of Testing and Methods, 2015 "ASTM Standard E139 Test Method for Conducting Creep, Creep-Rupture, and Stress-Rupture Tests of Metallic Materials," ASTM International, West Conshohocken, PA.
[23] ASTM E83-16, "Standard Practice for Verification and Classification of Extensometer Systems", ASTM International, West Conshohocken, PA, 2016.
[24] Stewart, C. M., 2013, "A Hybrid Constitutive Model for Creep, Fatigue, and Creep-Fatigue Damage," University of Central Florida.
[25] Haque, M. S., 2015, "An Improved Sin-Hyperbolic Constitutive Model for Creep Deformation and Damage," The University of Texas at El Paso.
[26] Haque, M. S., and Stewart, C. M., 2016, "Finite-Element Analysis of Waspaloy Using Sinh Creep-Damage Constitutive Model Under Triaxial Stress State," J. Press. Vessel Technol. Trans. ASME, 138(3), pp. 1–9.
[27] Haque, M. S., and Stewart, C. M., 2016, "Exploiting Functional Relationships Between MPC Omega, Theta, and Sine-Hyperbolic Continuum Damage Mechanics Model," *Proceedings of ASME 2016 Pressure Vessels and Piping Conference PVP 2016*, Vancouver, British Columbia, Canada, pp. 1–11.

